34th Annual International Conference of the IEEE EMBS
San Diego, California USA, 28 August - 1 September, 2012

Continuous Neural Decoding of Grasp Types for Asynchronous Brain Machine Interfaces*

Yaoyao Hao, Weidong Chen, Shaomin Zhang, Qiaosheng Zhang, Bo Jiang, Ting Zhao, Xiaoxiang Zheng

Abstract—**Decoding grasp types instead of individual finger kinematics from neural signals is an efficient way for prosthetic hand control in brain machine interfaces (BMIs). However, current grasp type decoding mainly depends on a synchronous way, i.e. the decoding has to be triggered by external events such as movement onset, making it less practical for BMI applications. This paper presents our work on asynchronous decoding of four grasp types and a resting state using neural ensemble signals from the primary and premotor cortex of a monkey. A fuzzy k-nearest neighbor and finite state machine were employed to continuously predict the movement states and onset timing of the hand motion when monkey grasping one of four different objects with specific gestures. Sample-wise and event-wise analyses were conducted to evaluate the performance of the system. The results demonstrate that it is possible to asynchronously decode grasp movement with a high accuracy, suggesting its potential application in practical BMIs.**

I. Introduction

The loss of the hand results in a serious reduction of the functional autonomy of a person in his daily living. In past decades, brain machine interfaces (BMIs) have provided a new hope for restoring motor functions of the severely disabled through controlling prostheses (e.g. robotic arm, screen cursor, etc.) with intentional commands extracted from brain signals [1, 2]. With the development of understanding how reach and grasp movements are encoded in distinct brain regions (for a latest review, see [3]), recent studies have paid attentions to the more sophisticated hand movement restorations by decoding distinct grasp types from cortical signals. Grasp types were classified successfully from multiunit activity (MUA) in dorsal and ventral premotor (PMd and PMv) [4], single neuron recording in PMv [5], multiple units in PMv and anterior intraparietal (AIP) [6], and even human Electrocorticographic (ECoG) [7] previously. These works, classifying finger configurations into one of the predefined categories based on the kinematic synergy movement in grasping, reduce the burden of the decoding system dramatically compared with continuous kinematic modeling.

Current decoding, however, always operated in a so-called synchronous or cue-based mode, in which human intervention is required to notify the decoder when it is appropriate to decode. The system used a priori knowledge of the movement events, which is not available in practical neuroprosthetic control [8]. In contrast, an asynchronous BMI, working in functional autonomous mode, decodes the continuous signal and gives out the results every moment depending on the subject's cognitive state [9]. Although this had not been applied to grasp decoding, there is some relevant work in the BMI field. Townsend et al. used asynchronous decoding to analyze continuous EEG data during right/left motor imagery, and introduced a resting states corresponding to non-intended activity [10]. Hasan et al. temporal modeled the EEG during self-paced hand movement, which are further used for building an onset detection system [11]. Kemere et al. detected the neural-state transitions among base-line, plan, and perimovement epochs of neural activity using hidden Markov models [12].

In this study, we obtained neural data from the primary motor and dorsal premotor cortices (M1 and PMd) of a monkey and decoded four grasp types and a resting state asynchronously for neural prosthetic control. Both sample-wise and event-wise analyses show that the movement states and movement onset timing can be classified accurately solely based on neural data without non-neural cue.

II. Materials and Methods

A. Experimental setup

We trained a male macaque monkey to reach and grasp four differently shaped objects using the right hand with different types of grasp. As illustrated in Fig. 1A, the four objects were fixed and randomly arranged in a two-by-two matrix on a transparent plexiglass board, which was located vertically in front of the animal at the chest level. The distance from the board to the eye of the animal was ~50 cm. An LCD monitor was mounted behind the board to illuminate one of the objects as the target for grasp. As shown in Fig. 1B, the four objects used in the task include a cylinder, a rectangle plate, a cone and a ring. Each object is small enough to be held in one hand of the monkey with a distinct grasp type. Specifically, the grasp types for the four objects are: heavy wrap for the cylinder, primitive precision for the plate, lateral grip for the cone and two-finger hook grip for the ring.

The monkey was seated in a primate chair with his head fixed and right arm resting on clapboard. As shown in Fig. 1C, a trial was initiated after one of the objects was randomly

* Resrach supported by grants from the National Natural Science Foundation of China (No. 61031002, 61001172), National High Technology Research and Development Program of China (No. 2012AA011602), Zhejiang provincial key science and technology program for international cooperation (No. 2011C14005).

Xiaoxiang Zheng is with Qiushi Academy for Advanced Studies, Department of Biomedical Engineering, Zhejiang University, HangZhou, China. (Corresponding author, phone: +86-571-87952838; fax: +86-571-87952865; e-mail: qaas@zju.edu.cn).

Yaoyao Hao, Qiaosheng Zhang, Bo Jiang, Ting Zhao and Shaomin Zhang are with the Qiushi Academy for Advanced Studies, and the Department of Biomedical Engineering, Zhejiang University, Hangzhou, China. (e-mail: hyy2046@163.com)

Weidong Chen is with Qiushi Academy for Advanced Studies, Department of computer Science, Zhejiang University, Hangzhou, China. (chenwd@zju.edu.cn)

illuminated by the light projected from the background screen (hereafter refer to Light ON). In each trial, the monkey was required to reach and grasp the object within 600 ms, and hold it for 3 to 4 seconds until the background screen light was turned off (hereafter refer to Light OFF). The monkey released the object and withdrew the hand to the rest position. A trial was considered successful if the monkey grasped the object in the intended sequence and grip type, and then several drops of water were rewarded to the animal manually. Several blocks (10 minutes each block, including ~50 trials) were conducted in one session, with a few minutes break between blocks. Hand and arm movement was also recorded using an infrared camera.

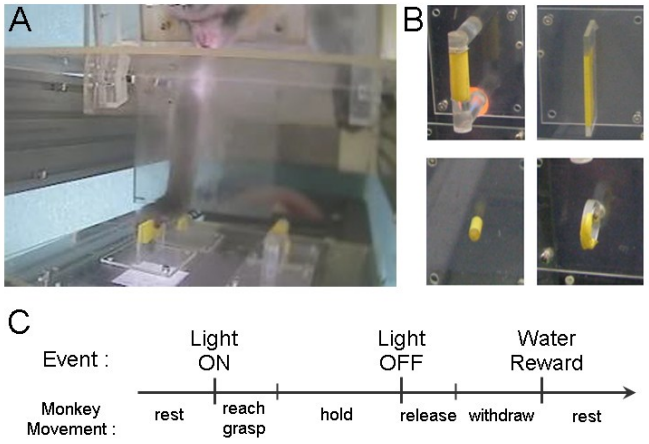

Figure 1. Experimental setup and task. (A) The top view of the experimental setup when monkey was grasping the plate. (B) The four target objects: cylinder, plate, cone and ring. (C) The time sequence of a single trial.

B. Neural recordings and preprocessing

Neural data was collected from two Utah microelectrode arrays (Blackrock, 96 channels) chronically implanted in the hand area of primary motor cortex (M1) and dorsal premotor cortex (PMd) contralateral to the hand performing the task. Surgical procedure was similar to those described in [13]. All experimental procedures in this study conformed to the Guide for the Care and Use of Laboratory Animals (China Ministry of Health) and were approved by the Animal Care Committee at Zhejiang University, China.

Continuous neural activities were recorded from the first 64 channels (out of 96) from each array in M1 and PMd using a 128-channel Cerebus Data Acquisition system (Blackrock, USA). Signal from each channel was amplified, analog filtered (Butterworth bandpass, 0.3-7500 Hz), digitized (14 bit resolution, 30 kHz sample) and digitally filtered (Butterworth highpass at 250 Hz). Spike activities were detected from the filtered signal using the thresholding method at a level of -5.5 times the root mean square (RMS) of signal baseline. Online spike sorting was conducted using template labeled with hoop method. Event timing, including trial start, Light ON, Light OFF, trial end and reward, were also recorded via the digital input port of the system synchronously. These data were stored on disk for offline analysis.

C. Decoding method and control strategy

The numbers of spikes for each sorted unit were counted in 100 ms bins across the entire trial, which results in the neural vectors along the grasp movement. The time course of whole movement was first labeled as *Grasp* state and *Rest* state, roughly corresponding to the periods between and beyond Light ON and Light OFF event, respectively. The *Grasp* state was further classified as four types of grip according to the object grasped. Fuzzy k-nearest neighbors (FKNN) was used to classify the five movement states continuously in this application [14]. Given a training set D = [y_1, y_2, ... y_n] with n labeled samples and a test neural vector z related to one of the five states with unknown class label, the algorithm computes the distance between z and all the training samples to determine its k nearest-neighbor list. It then assigns a fuzzy membership vector (FMV) to the testing vector. The FMV is defined as M = [m_1, m_2, ... m_L], where L is the number of classes and m_i denotes the membership to the *i-th* class, i.e. *class(i)*. m_i is calculated as:

$$m_i = \sum_{y \in class(i)} \frac{1}{\|z-y\|} \Big/ \sum_{y \in Neighbor} \frac{1}{\|z-y\|} \qquad (1)$$

Then the unlabeled vector z will be classified into *class(i)*, where m_i is the maximum value within the FMV.

We calculated the labels (i.e., movement states) in each trial bin by bin along the whole time course of grasp. A finite state machine (FSM) was designed in this application which can convert the output labels of the FKNN classifier to the primitive prosthetic hand control commands asynchronously. For stable and smooth operation of the control, we designed a set of state transition polices. First, if no membership predicted from FKNN was above a predefined threshold, the FSM regarded it as ambiguous and kept the current state unchanged. Second, FSM transited to a new state only when the classification label of the state was predicted in 5 consecutive bins. Third, the state cannot transfer from one kind of grasp type to another directly; *Rest* state must be inserted, which is also the actual situation. Only when the output state of the FSM changed, the command of grasping or releasing was sent. In practice, the FSM output was smoother than the FKNN output, and the former was used for further analysis and statistics.

III. RESULTS

The goal of this work is to discriminate different movement states asynchronously along the time course of reach and grasp. Monkey was trained to grasp one of the objects when the corresponding light is on and release it when the light is off. A total of 128-channel neural signals in M1 and PMd were obtained from 10 sessions over a period of one month. After sorting, we isolated an average of 73 units per session. The performance of the system was evaluated offline by several criteria.

Fig.2 shows some example neurons and their firing rate during one session's reach and grasp time course. ON and OFF are corresponding to the event of Light ON and Light OFF, respectively. Neuron 113-2 and 53-2 are responsive to reach and withdraw movement, regardless of different objects. Neuron 86-1 and 91-1 are sensitive to different objects grasp, i.e., for different objects they show different firing rate during the grasp and hold movement. These tuning properties provide the basis of the asynchronous decoding, in which, both reach timing and grasp type are predicted.

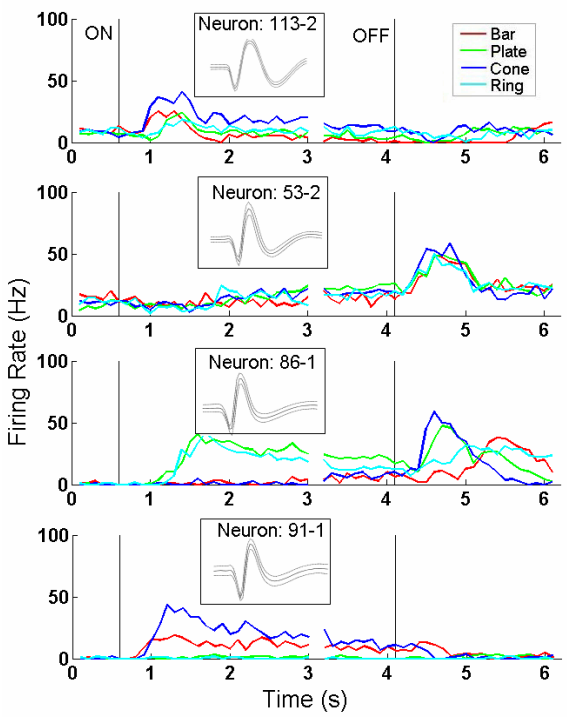

Figure 2. Example neurons showing different reach grasp tuning property.

A. *Bin-wise result*

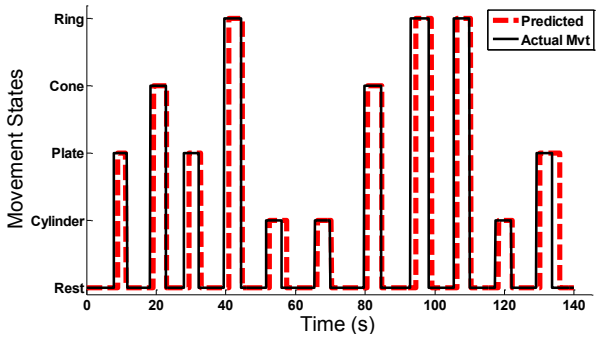

Figure 3. Representative bin by bin decoding results showing actual movement sequence and the predicted counterpart in 11 successive trials.

Representative result of bin-wise decoding, which predicts the state of movement from each bin of the neural signals, is shown in Fig. 3. The prediction of the FSM is compared with actual movement synchronously. The start and end of the four objects grasp was calibrated as the event timing of Light ON and Light OFF respectively. In the tested trials illustrated, the predicted movement followed the actual movement of the monkey completely: (i) the four grasp types were predicted correctly; (ii) the rest state was also predicted correctly; and (iii) the predicted grasping and releasing timing was corresponding to the actual movement sequence, only with a little delay. To evaluate the bin-wise prediction accuracy across all the sessions, receiver operating characteristics (ROC) curve was plotted with true positive rate (TPR) against false positive rate (FPR) in Fig. 4. The TPR and FPR are defined as:

$$TPR = TP/(TP+FN) \tag{2}$$

$$FPR = FP/(TN+FP) \tag{3}$$

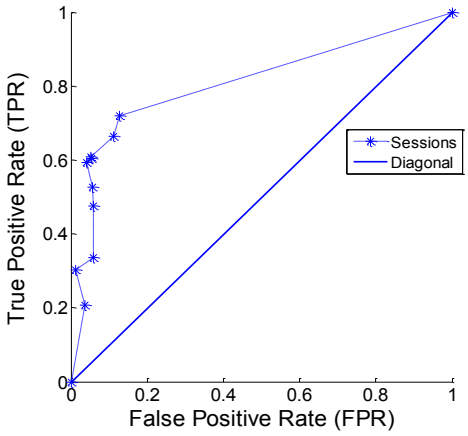

Figure 4. ROC curve generated on a bin by bin comparison of the classifier output against the actual movement across all the sessions.

where TP, FN, TN and FP are the number of true positives, false negatives, true negatives and false positives, respectively. Here, grasp movements are taken as a positive signal and rest state as a negative signal. The averaged TPR and FPR across all 10 sessions are 0.54 (standard deviation, SD, 0.17) and 0.07 (SD, 0.04), respectively. The area below the ROC curve, giving a measure about the mean separability in all the sessions, was evaluated at a high level of 0.81. The delay between actual movement onset and predicted onset was evaluated at an average of 587 ms (SD, 237 ms) across all the correctly classified trials. The delay was mainly due to the policy of using 5 consecutive bins for making a decision.

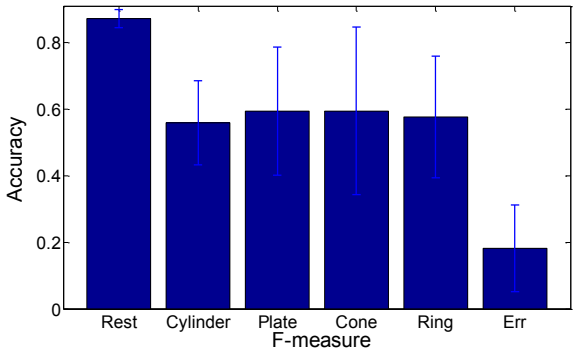

Figure 5. Mean F-measure values of the five movement states and the comprehensive error rate across all the sessions.

Additionally, an F-measure (i.e., balanced F-score) is used to check the classification performance of the individual classes as in [11]. The F-measure for a certain class c is defined as the harmonic mean of precision and recall:

$$F_c = 2 \times \frac{\mathrm{Precision}_c \times \mathrm{Recall}_c}{\mathrm{Precision}_c + \mathrm{Recall}_c} \tag{4}$$

where

$$\mathrm{Precision}_c = TP_c/(TP_c + FP_c) \tag{5}$$

$$\mathrm{Recall}_c = TP_c/(TP_c + FN_c) \tag{6}$$

where TP, FP and FN are defined above. Another quantitative measurement is defined as an error function as fellow:

$$Err = \sum_{c=1}^{C} (1 - F_c)^2 / C \quad (7)$$

where C is the total number of classes (i.e. 5 in this work). The error function gives a comprehensive evaluation of F-measure under the numbers of classes in term of error rate. Fig. 5 details the F-measure values of the five movement states, in which, the value of *Rest* states (mean, 0.87; SD, 0.02) is significantly higher than other grasp movements (student t-test, $p < 0.01$), showing a classification bias towards *Rest* states. While the other four grasp movement states show a balanced performance, indicating that the subject has no preference to any objects. The average error defined in (7) was 0.18 (SD, 0.13), which is a low error indicator for the whole classifier system performance.

B. Event-wise result

Event-wise decoding predicts the movement state for each grasp event, which is defined as a complete period of grasping. It is a more practical strategy for real BMI applications than bin-wise analysis because a grasping action is usually completed without interruption. Here event is defined as one grasp in one trial and the rest state is defined as non-event. The numbers of true-positive events (TPE) and false-positive events (FPE) are counted to measure the performance. Here TPE is defined as both grasp and rest states were predicted correctly in one trial, i.e., only one continuous period of the correct decoding result appeared in each state (single detection), and FPE is defined as any artifact grasp movement detection in rest periods. A new true-false difference (TF%) is defined as the difference in the ratio of TPEs to events and FPEs to tests in [10], compared with the traditional true-false difference (trTF%):

$$trTF\% = (TPE - FPE) / E \quad (8)$$

$$TF\% = TPE / E - FPE / (E + FPE) \quad (9)$$

where E is the total number of events (i.e. trials). The TF difference will be 1 if there is detection for each event and no detections during nonevent. For a detection system with random behavior, these two parameters will both be 50%, giving a TF difference of zero. The event by event results are summarized in Table I. In a total of 651 trials tested, the mean TPE and FPE are 584 and 77 respectively, which result in a mean TF difference of 0.75 (SD, 0.14). Specially, a total of 143 (out of 146) trials was predicted correctly and only 6 false alarm occurred in session 7, which is also the data used in Fig. 3. The traditional TF difference gives the similar evaluation.

TABLE I. EVENT BY EVENT EVALUATION OF THE SYSTEM PERFORMANCE ACROSS ALL THE SESSIONS IN TRUE-FALSE DIFFERENCE

Session	TPEs	FPEs	Events	trTF%	TF%
1	31	8	38	0.61	0.64
2	56	7	60	0.82	0.83
3	63	6	63	0.90	0.91
4	40	4	58	0.62	0.62
5	24	5	38	0.50	0.52
6	71	13	71	0.82	0.85
7	143	6	146	0.94	0.94
8	74	9	82	0.79	0.80
9	50	13	54	0.69	0.72
10	32	6	41	0.63	0.64
Mean	58.4	7.7	65.1	**0.73**	**0.75**
Std	34.3	3.1	31.8	**0.14**	**0.14**

IV. CONCLUSION AND DISCUSSION

Asynchronous decoding of monkey reach and grasp movement was realized successfully in this study with a high accuracy of bin-wise and event-wise evaluation, which means that both different movement states and movement onset timing were predicted exactly. One of the main limitations in this work is that the start and end of the four objects grasp was calibrated as the event timing of Light ON and Light OFF respectively which may not be equal to the actual onset of movement. To precisely detect the onset of the grasp movement, an analysis of the video recordings or a marker based movement analysis has to be performed.

The output of the system can be used to control an artificial hand or a hand in virtual reality using the shared control strategy, i.e. when the output state of the FSM changed, a corresponding grasp/release primitive command was sent to the hand and the hand will act accordingly. Future work includes implementing more movement states such as reach, release, drawback, etc. and employing more complicated states model to simulate the reach and grasp movements.

REFERENCES

[1] M. Velliste, S. Perel, M.C. Spalding, A.S. Whitford, and A.B. Schwartz, "Cortical control of a prosthetic arm for self-feeding", *Nature*, vol. 453, pp. 1098-1101, 2008.

[2] L.R. Hochberg, M.D. Serruya, G.M. Friehs, J.A. Mukand, M. Saleh, A.H. Caplan, A. Branner, D. Chen, R.D. Penn, and J.P. Donoghue, "Neuronal ensemble control of prosthetic devices by a human with tetraplegia", *Nature*, vol. 442, pp. 164-171, 2006.

[3] S.T. Grafton, "The cognitive neuroscience of prehension: recent developments", *Exp Brain Res*, vol. 204, pp. 475-91, 2010-08-01 2010.

[4] E. Stark and M. Abeles, Predicting movement from multiunit activity, J Neurosci, vol. 27, (no. 31), pp. 8387-8394, 2007.

[5] J. Carpaneto, M.A. Umilta, L. Fogassi, A. Murata, V. Gallese, S. Micera, and V. Raos, "Decoding the activity of grasping neurons recorded from the ventral premotor area F5 of the macaque monkey", *Neuroscience*, vol. 188, pp. 80-94, 2011.

[6] B.R. Townsend, E. Subasi and H. Scherberger, "Grasp movement decoding from premotor and parietal cortex", *J Neurosci*, vol. 31, pp. 14386-98, 2011.

[7] T. Pistohl, A. Schulze-Bonhage, A. Aertsen, C. Mehring, and T. Ball, "Decoding natural grasp types from human ECoG", *Neuroimage*, vol. 59, pp. 248-60, 2012.

[8] V. Aggarwal, S. Acharya, F. Tenore, H.C. Shin, R. Etienne-Cummings, M.H. Schieber, and N.V. Thakor, "Asynchronous decoding of dexterous finger movements using M1 neurons", *IEEE Trans Neur Sys Reh*, vol. 16, pp. 3-14, 2008.

[9] S.G. Mason and G.E. Birch, "A brain-controlled switch for asynchronous control applications", *IEEE Trans Biomed Eng*, vol. 47, pp. 1297-307, 2000.

[10] G. Townsend, B. Graimann and G. Pfurtscheller, "Continuous EEG classification during motor imagery--simulation of an asynchronous BCI", *IEEE Trans Neural Syst Rehabil Eng*, vol. 12, pp. 258-65, 2004.

[11] B.A. Hasan and J.Q. Gan, "Temporal modeling of EEG during self-paced hand movement and its application in onset detection", *J Neural Eng*, vol. 8, pp. 056015, 2011.

[12] C. Kemere, G. Santhanam, B.M. Yu, A. Afshar, S.I. Ryu, T.H. Meng, and K.V. Shenoy, "Detecting neural-state transitions using hidden Markov models for motor cortical prostheses", *J Neurophysiol*, vol. 100, pp. 2441-52, 2008.

[13] S. Suner, M.R. Fellows, C. Vargas-Irwin, G.K. Nakata, and J.P. Donoghue, "Reliability of signals from a chronically implanted, silicon-based electrode array in non-human primate primary motor cortex", *IEEE Trans Neur Sys Reh*, vol. 13, pp. 524-541, 2005.

[14] J.M. Keller, M.R. Gray and J.A. Givens, "A Fuzzy K-Nearest Neighbor Algorithm", *IEEE Tran Sys, Man, and Cyber*, vol. 15, pp. 581, 1985.